

Chimera states in ring-star network of Chua circuits

Sishu Shankar Muni* Astero Provata †

August 6, 2020

Abstract

We investigate the emergence of amplitude and frequency chimera states in ring-star networks consisting of identical Chua circuits connected via nonlocal diffusive, bidirectional coupling. We first identify single-well chimera patterns in a ring network under nonlocal coupling schemes. When a central node is added to the network, forming a ring-star network, the central node acts as the distributor of information, increasing the chances of synchronization. Numerical simulations show that the radial coupling strength k between the central and the peripheral nodes acts as an order parameter leading from a lower to a higher frequency domain. The transition between the domains takes place for intermediate coupling values, $0.5 < k < 2$, where the frequency chimera states prevail. The transition region (width and boundaries) depends on the Chua oscillator parameters and the network specifics. Potential applications of star connectivity can be found in the control of Chua networks and in other coupled chaotic dynamical systems. By adding one central node and without further modifications to the individual network parameters it is possible to entrain the system to lower or higher frequency domains as desired by the particular applications.

1 Introduction

Chimera states are characterized by the coexistence of synchronous and asynchronous areas when identical dynamical units are coupled equivalently in some network topology. Most commonly studied are the frequency chimeras, which are distinguished by the difference in frequency of the oscillatory elements. Although all oscillators have the same intrinsic frequency, it is the coupling between them which creates a distribution of frequencies in the network, a reason

*School of Fundamental Sciences, Massey University, Palmerston North, New Zealand

†Institute of Nanoscience and Nanotechnology, National Center for Scientific Research "Demokritos", 15341 Athens, Greece

Keywords: Chimera states, Chua circuit, nonlocal diffusive coupling, ring-star network

E-mail addresses: S.S. Muni (s.muni@massey.ac.nz)

A. Provata (a.provata@inn.demokritos.gr)

why the chimera states are nontrivial and unexpected. Kuramoto and Battogtokh first observed these patterns in nonlocally coupled phase oscillators described in [1, 2]. Following these first reports, chimera states have been studied extensively during the past two decades. Researchers found chimera states in many different types of dynamical systems, like coupled phase oscillatory flows and discrete maps connected in different network topologies and coupling forms, as described in recent review articles [3, 4, 5, 6]. Besides the typical chimeras as reported by Kuramoto, where the synchronous and asynchronous domains remain fixed in space, more complex chimera patterns were recently reported, such as breathing chimeras, alternating chimeras [7], spiral wave chimeras [8], amplitude chimeras [9], and many more.

Applications of chimera states were first reported in systems of coupled nonlinear neuronal oscillators [5]. These oscillators are known to exhibit highly nonlinear behavior and chimera states were found in systems that mimic the neuronal activity like the FitzHugh-Nagumo (FHN), the Hindmarsh-Rose (HR), and the Hodgkin-Huxley (HH) systems [10, 11, 12, 13]. Apart from the numerical studies, experimental evidence of chimera states related to neuronal activity has also been reported in [14], in which nine FHN oscillators in a ring were considered. Synchronization/coordination aspects related to neurological disorders like epilepsy were studied via this system. The results indicated that epilepsy is not only a dynamical disease but also a topological disease that depends on the type of connection between the neurons. Further indications on the presence of chimera states at the onset of epileptic seizures are reported in references [15, 16, 17]. It has also been claimed that chimera states are deeply connected with the causes of creating various kinds of neuronal diseases like Parkinson's disease, schizophrenia, brain tumors, etc [18]. While performing experiments, Tognoli et al. reported in reference [19] the presence of synchronous and asynchronous activity during left and right finger movements. Also in relation to brain activity, chimera states have been associated with the unihemispheric sleep pattern in aquatic creatures and birds, where they sleep with one eye open leading one half of the brain in the synchronous state and the other half in the asynchronous [20, 21, 22].

Besides experiments related to neuronal activity, experimental evidence of chimera states have been reported in diverse disciplines and notably in the domains of mechanical oscillators [23], coupled map lattices [24], nonlocally coupled FitzHugh-Nagumo and Stuart-Landau oscillator circuits [25, 26] and chemical oscillators [27, 28, 29]. Recent numerical evidence indicates that metamaterials are also a promising domain for chimera applications [30, 31]. Apart from the confirmation of the chimera states in experiments and simulations, it still remains an open problem to deal analytically with the mechanism behind the formation of these hybrid states and their control, making the study of chimeras an active research area.

The Chua circuit is considered as the simplest nonlinear circuit to exhibit chaotic behavior [32]. It is composed of an inductor, two capacitors, a resistor, and a Chua diode. The circuit's temporal evolution is described by a three dimensional continuous dynamical system. The Chua diode, being a nonlinear

local active resistor, is mainly responsible for the chaotic behavior of the circuit, which is well known for its double-scroll attractor [33]. Regarding applications, Chua circuits are used in secure communications [34], in improving performance of ultrasonic devices in the presence of cross talk [35] and in the generation of Gaussian, white noise which is essentially useful in many engineering systems [36]. Other applications include Avant-Garde music compositions [37], storage of analog patterns and managing the problem of handwritten recognition [38]. Many present-day applications of the Chua circuit are described in reference [39].

Star networks and ring networks are usually common in social systems, hubs, social networks, computer networks [40]. In the latter, the information flow needs to be transmitted securely, else there is a compromise in the security leading to cybercrimes. Chua circuits connected in the computer networks, in particular, can help in achieving secure communications as the Chua circuits have proven to be useful in many cryptographic systems [41].

Synchronization of Chua oscillators was studied in star networks and their properties were established using different kinds of coupling, such as diffusive, conjugate and mean-field couplings [42]. The regimes of full synchronization of the Chua oscillator networks were mainly studied using these different coupling forms. A variety of chimera structures have been reported in the case of Chua circuits connected in a ring [43]. Chimera states were also observed in the star network consisting of synchronized and desynchronized oscillators in the group. In a two-dimensional lattice of Chua oscillators, spiral waves are obtained in [44]. The present study is an extension of the previous work [42], in the sense that we are using a composite connectivity scheme: starting with a ring of Chua circuits with nonlocal connectivity and common coupling strength σ (see [43]), we apply an additional radial connectivity where every Chua circuit is bidirectionally connected to a central node with a variable coupling strength k . By varying the values of k and σ we can transit from a pure ring connectivity, when $k = 0$ and $\sigma \neq 0$, to a pure star (central) connectivity, when $k \neq 0$ and $\sigma = 0$. We investigate the prevalence of different chimera patterns in this composite connectivity, which we refer to as the ring-star Chua network.

In particular, in this study starting from the pure ring connectivity with non-local coupling we recover the chimera structure known as single-well chimera as shown in reference [43]. To set terminology, here we need to explain the difference between multi-scroll attractors, such as the Chua attractors, and multi-level chimeras. A multi-scroll attractor represents the phase space of a single chaotic oscillator, whose trajectory circulates in the vicinity of multiple regions, escaping occasionally from each of these regions to the others [32]. Chimera states, on the other hand, are formed in systems of many coupled oscillators, where domains of coherent and incoherent oscillators are formed. In chimera states the coupled oscillators can be chaotic or simpler limit cycles. When the coupled elements have complex phase space, multiple domains of synchronized elements are formed, separated by domains where the oscillators are asynchronous. These are called multi-well chimeras and consist of regions (wells) of coherent elements with constant common frequencies, separated by incoherent regions where the

oscillators develop different frequencies [43]. In the present study, by turning on the radial coupling k , we show that initially, the single-well chimera structures persist in the ring-star network and all oscillators have specific low frequencies. As k increases, there is an abrupt transition at finite k -values, where the system passes from the low frequency regime to a high frequency regime, passing by the intermediate k -region where domains of high and low frequencies co-exist. The k -value where the transition occurs depends on the ring coupling strength σ .

In the following, when we refer to the exchange of information between nodes i and j in the system, we mean that at a certain time t the state variables $x_i(t)$ and $y_i(t)$ of node i receive and use the values of the state variables $x_j(t - \Delta t)$ and $y_j(t - \Delta t)$ of node j in the previous time step $t - \Delta t$. This must not be confused with the notion of global information, energy or entropy exchange between the nodes as discussed in the literature of synchronization between interacting units [45, 46, 47, 48, 49, 50, 51] and more recently on synchronization in the form of chimera states [52, 53].

The transitions from asynchronous patterns to chimera states and to synchronized states are quantitatively studied with the help of the different synchronization measures [54]. The mean phase velocity [55] is a common measure considered to demonstrate the presence of chimera structures. However, it frequently fails to identify them, mainly in the cases of traveling or diffusing chimeras. In those cases, there is a need for different measures to be considered, which can work as alternatives to the mean phase velocity. Alternative measures analyzing the relative size of the coherent/incoherent domains, the degree of coherence etc were considered in [54]. We establish the chimera kingdom in the ring-star network of Chua circuits using these measures, to avoid the problems of pattern displacement in space and for quantitative comparison between the different chimera morphologies.

The paper is organized as follows: Section 2 introduces the Chua circuit and the ring-star network topology. In a separate subsection, 2.1, the various synchronization measures are introduced. Section 3 discusses the simulation results obtained in the case of Chua circuits coupled in a ring geometry for parameter values where single-well chimeras emerge. Section 4 is devoted to the ring-star network connectivity. The deformation of the single-well chimeras as a function of the radial coupling k is discussed in this section. In section 5 the transition of the system from the lower frequency to the higher frequency domain is discussed where the frequency chimera states prevail. In all cases, alternative synchronization measures are considered for the quantitative study of the mean phase velocity profiles. In the conclusions the main results of this study are recapitulated and some challenges ahead in analyzing the ring-star network are proposed.

2 Chua ring-star network model

A sketch of the ring-star network is shown in Figure 1. A number of N Chua oscillators are connected in a ring-star network with nonlocal diffusive coupling. Oscillators are indexed as $i = 1$ for the central node and $i = 2, \dots, N$ for the peripheral (end) nodes. The central node ($i = 1$) is connected to all the peripherals with the same coupling strength k . Each peripheral oscillator is nonlocally connected to R nodes to its left and R nodes to its right with common coupling strength σ and is also linked to the central node with coupling strength k . To enforce uniformity of the end nodes, periodic boundary conditions are considered.

The dynamical equations of the ring-star network are given by Eqs. (1) and (2). For $i = 2, \dots, N$, the dynamical equations of the end nodes are given by:

$$\begin{aligned} \dot{x}_i &= f_x + k(x_1 - x_i) + \frac{\sigma}{2R} \sum_{k=i-R}^{k=i+R} (x_k - x_i), \\ \dot{y}_i &= f_y + \frac{\sigma}{2R} \sum_{k=i-R}^{k=i+R} (y_k - y_i), \\ \dot{z}_i &= f_z. \end{aligned} \tag{1}$$

For $i = 1$ (central node) the dynamical equations are:

$$\begin{aligned} \dot{x}_1 &= f_x + \sum_{j=1}^N k(x_j - x_1), \\ \dot{y}_1 &= f_y, \\ \dot{z}_1 &= f_z. \end{aligned} \tag{2}$$

where

$$\begin{aligned} f_x &= \alpha(y_i - x_i - (Bx + \frac{1}{2}(A - B)(|x + 1| - |x - 1|))), \\ f_y &= x_i - y_i + z_i, \\ f_z &= -\beta y_i. \end{aligned}$$

with periodic boundary conditions:

$$\begin{aligned} x_{i+N}(t) &= x_i(t), \\ y_{i+N}(t) &= y_i(t), \\ z_{i+N}(t) &= z_i(t). \end{aligned}$$

for $i = 2, 3, \dots, N$. Following references [42, 43], we have used coupling only in the x and y -variables and not in the z -variable of the Chua coupled elements. Similar coupling only via one variable is used in reference [56] for coupled Rössler oscillators.

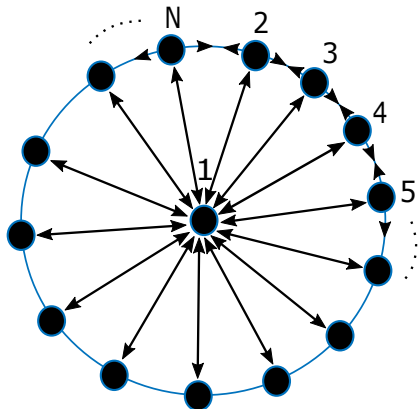


Figure 1: The Chua ring-star network. Here we consider $N = 300$ Chua circuits where the central one is labeled $i = 1$ and the end nodes are labeled from $i = 2, \dots, N$.

From the interaction scheme, it is now clear that oscillators $i = 2, \dots, N$ exchange information via their x - and y -variable with $2R$ neighbors symmetrically set around i , while the central unit $i = 1$ exchanges information with all other units $j = 2, \dots, N$ (also via their x - and y -variables only). Due to the Euler integration scheme used, the variables $x_i(t), y_i(t), z_i(t)$ are updated using the values $x_i(t - \Delta t), y_i(t - \Delta t), z_i(t - \Delta t)$ at the previous time step, as also stated in the Introduction.

As working parameter set the following values are used throughout this study: The parameters of the identical Chua circuits are set to $A = -1.143$, $B = -0.714$, $\alpha = 9.4$ and $\beta = 14.28$ in order to keep the circuit in the oscillatory, double-scroll regime. The system size is set to $N = 300$ and the coupling range to $R = 100$. The rest of the parameters, the coupling strength σ between the peripheral nodes, and the coupling strength k between the central node and the peripheral ones are varied to explore their influence in the network synchronization patterns.

2.1 Synchronization measures

As discussed in the Introduction, the mean phase velocity or average frequency ω is a valuable measure to quantify the synchronization of the oscillators [55]. For the i -th oscillator, the mean phase velocity is denoted by ω_i . For a large computational time interval T , ω_i expresses the number of times the variable x_i crosses a certain fixed constant value, say c . If the variable x_i crosses the constant c , M_i times with positive slope, then the mean phase velocity of the i -th oscillator is calculated as :

$$\omega_i = \frac{2\pi M_i}{T} = 2\pi f_i. \quad (3)$$

The positive slope considered in the counting of M_i in Eq. (3) is needed to avoid double counting the number of periods calculated within the time interval T . The quantity f_i denotes the average frequency, which differs from the mean phase velocity by a factor 2π . Due to this simple relation, in the following the terms “mean frequency” and “mean phase velocity” will be used interchangeably.

Chimera states are characterized by the difference in frequency of the identical oscillatory circuit elements. The coupling is responsible for the change in frequency in some oscillators. This is the reason why the chimera states are so nontrivial and unexpected. Different synchronization measures come to play as additional quantitative indices when inconclusive information is conveyed by the mean phase velocity. Such synchronization measures were discussed in [54]. We complement our work with the computation of the relative size of the incoherent and coherent parts denoted by r_{incoh} and r_{coh} , respectively. Let us denote by ω_{coh} the common mean phase velocity of the coherent elements, by ω_i the mean phase velocity of the i -th oscillator and by N the number of oscillators considered. The quantity r_{coh} is defined as :

$$r_{coh} = \frac{1}{N} \sum_{i=1}^N \chi(A_1) \quad (4)$$

where χ is a step function which returns 1 if A_1 is positive and returns 0 if A_1 is negative. A_1 is defined as:

$$A_1 = \|\omega_i - \omega_{coh}\| - \epsilon \quad (5)$$

In definition (5) a small tolerance ϵ is added in order to take into account the fluctuations at the coherent level while computing r_{coh} according to Eq. (4).

Similarly, the quantity r_{incoh} is defined as :

$$r_{incoh} = \frac{1}{N} \sum_{i=1}^N \chi(A_2) \quad (6)$$

where

$$A_2 = \begin{cases} \omega_i - \omega_{coh} - \epsilon, & \omega_{coh} < \omega_{incoh}, \\ \omega_{coh} - \omega_i - \epsilon, & \omega_{coh} > \omega_{incoh} \end{cases} \quad (7)$$

Note that in the definition (7) two cases are considered. That is because one needs to cover both cases: when the ω_{coh} coincides with the minimum frequency in the system (upper case in Eq. (7)) and when the ω_{coh} coincides with the maximum frequency in the system (lower case in Eq. (7)). Both cases have been recorded in the literature on chimera states, see references [10, 54, 57]. In our simulations, the tolerance level ϵ is fixed to be $0.2\Delta\omega$, where $\Delta\omega = \omega_{max} - \omega_{min}$ is the difference between the maximum and minimum ω_i values in the system.

3 Chimera states in Chua ring networks

In this section, we study the case of a ring network where each element is a Chua circuit nonlocally linked to its neighbors, as was proposed and studied by

Shepelev et al. in reference [43]. Following [43] we consider here the formation of chimeras in the case of ring connectivity with nonlocal diffusive coupling. To avoid unnecessary complexity which arises in the parameter regions where the double-well chimeras prevail, we restrict ourselves in the parameter regions where only single-well chimera states are observed.

Starting with a ring network of $N = 300$ Chua oscillators with nonlocal diffusive coupling, we record single chimera states for different values of the network parameters (work by Shepelev et al. [43]). As an exemplary case, in Fig. 2 we record the spatial and temporal behavior of the network for coupling parameters $\sigma = 0.75$ and $k = 0$. Panel 2a depicts the spatial profile of the network at 25 snapshots at time intervals of 40 units. This figure depicts a single-well chimera state, where domains of alternating oscillatory properties are formed. Having started with initial conditions, $(x(t = 0), y(t = 0), z(t = 0))$, randomly distributed in the interval

$$[0 < x(t = 0) < 1, 0 < y(t = 0) < 1, 0 < z(t = 0) < 1],$$

the system remains always in the positive side of the axes (single-well) and all elements oscillate around the value $x = 1.5$, but amplitude variations are observed in the different domains formed. For clarity, a single snapshot is presented in panel 2b. The mean phase velocity, panel 2c, clearly identifies the domains where oscillators act coherently, and the incoherent domains.

In the next section, 4, we introduce a central node to the system, creating the ring-star network, and we investigate the system's response by varying the radial coupling strength k . We study the system response in the case of single-well chimeras, using as coupling constant parameter $\sigma = 0.75$ and variable k , as discussed above.

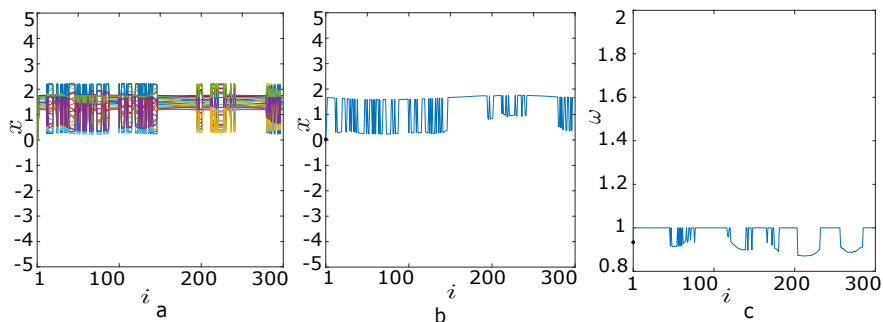


Figure 2: Ring network: Single-well chimera structures and measures for $\sigma = 0.75, k = 0$ with nonlocal diffusive coupling. a) 25 snapshots of the x_i -variables at time intervals of 40 units, b) typical single snapshot of the x_i -variables and c) mean phase velocities. Chua circuit parameters are $A = -1.143, B = -0.714, \alpha = 9.4, \beta = 14.28$ and network parameters are $N = 300$ and $R = 100$.

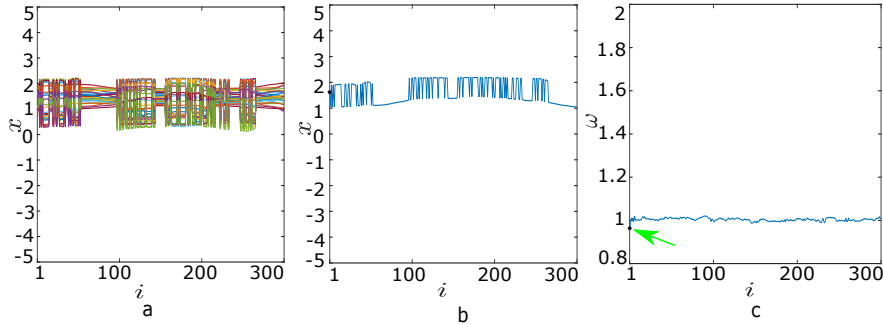


Figure 3: Ring-star network: Single-well chimera structures and measures for $\sigma = 0.75, k = 0.25$ with nonlocal diffusive coupling. a) 25 snapshots of the x_i -variables at time intervals of 40 units, b) typical single snapshot of the x_i -variables and c) mean phase velocities. The arrow in panel c) indicates the mean phase velocity of the central node. All other parameters as in Fig.2.

4 Chimera states in ring-star Chua networks

We now extend the Chua ring network model by adding a central node in the center of the ring which is linked equally to all the external nodes. We consider the mixed dynamics of the system and record its transition between chimera states and the full synchronization regimes. Simulations were carried out by considering random initial conditions for x, y, z state variables in the interval $[0, 1]$, as in previous section.

To investigate the influence of the central node in the Chua ring network we gradually vary the coupling strength k between the central node and the peripheral ones. All parameters of the identical Chua circuits are kept to the working parameter set, while the network contains $N = 300$ nodes and each Chua oscillator is connected to $R = 100$ neighbors to the left and $R = 100$ neighbors to the right. The ring coupling strength is fixed to $\sigma = 0.75$. [The pure-ring network briefly discussed in the previous section is equivalent to the case of $k = 0$ (no central node), while the ring-star network is realized when $k \neq 0$.]

The central node of the network plays a double role: First it receives “information” from the peripheral nodes and integrates it forming its own dynamics. Second, it redistributes the obtained information to the peripheral nodes, in such a way that each peripheral node receives information about the average (mean-field) dynamics of the ensemble of all peripheral nodes. Therefore, the central node acts as a modulator of the local dynamics using information over the ensemble dynamics. Based on this view of the system, we ask the question: How does the strength of the central coupling k influences the distribution of information and the overall synchronization properties of the network? To answer this question we performed numerical simulations using the same parameters as

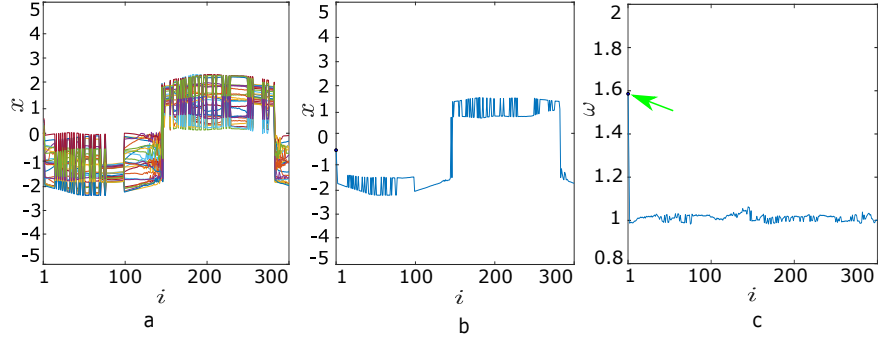


Figure 4: Ring-star network: Double-well chimera structures and measures for $\sigma = 0.75, k = 1$ with nonlocal diffusive coupling. a) 25 snapshots of the x_i -variable at time intervals of 40 units, b) typical single snapshot of the x_i -variable and c) mean phase velocities. The arrow in panel c) indicates the mean phase velocity of the central node. All other parameters as in Fig.2.

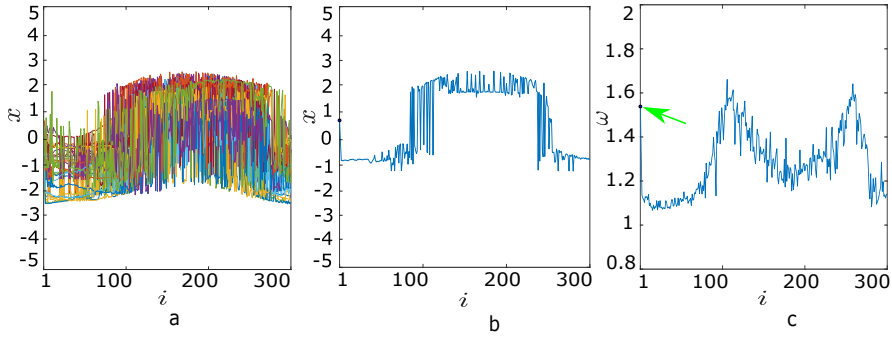


Figure 5: Ring-star network: Double-well chimera structures and measures for $\sigma = 0.75, k = 1.3$ with nonlocal diffusive coupling. a) 25 snapshots of the x_i -variables at time intervals of 40 units, b) typical single snapshot of the x_i -variables and c) mean phase velocities. The arrow in panel c) indicates the mean phase velocity of the central node. All other parameters as in Fig.2.

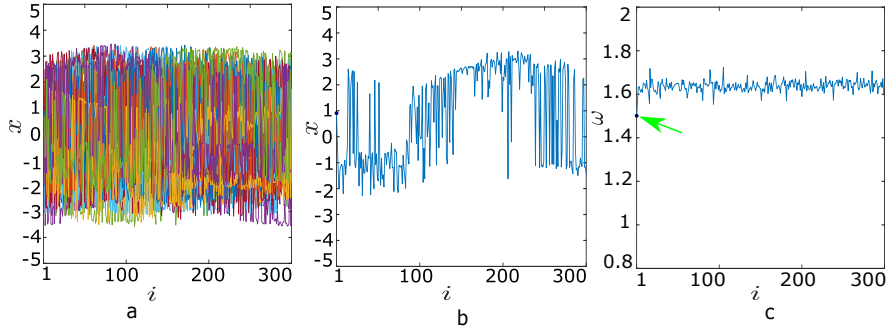


Figure 6: Ring-star network: Double-well chimera structures and measures for $\sigma = 0.75, k = 2.5$ with nonlocal diffusive coupling. a) 25 snapshots of the x_i -variables at time intervals of 40 units, b) typical single snapshot of the x_i -variables and c) mean phase velocities. The arrow in panel c) indicates the mean phase velocity of the central node. All other parameters as in Fig.2.

in the case of the single-well chimera and varied the central coupling parameter in the range $0 \leq k \leq 4$.

We provide below some examples of the modifications which take place when the central coupling strength k becomes nonzero. When a small deviation is applied leading from the ring network, $k = 0$, to the ring-star network, $k = 0.25$, as in Fig. 3, we observe that the single-well chimera persists: the x state variable keeps oscillating in the positive part of the axis and does not transverse below $x = 0$. For this low k -value, all oscillators have very similar frequencies, as can be seen in Fig. 3c. The green arrow in panel (c) points to the mean phase velocity ω_1 of the central node, which is slightly lower than the rest of the elements. Increasing the radial strength to $k = 1$ in Fig. 4 and $k = 1.3$ in Fig. 5, the single-well chimeras change to double-well ones. In both cases two domains of oscillators are formed: one domain where the x -variables oscillate in the positive axis and one in the negative axis. Related to the mean phase velocity values, in the case of $k = 1$, Fig. 4c, all peripheral nodes have the same mean phase velocity, while the central node has increased its mean phase velocity, $\omega_1 \sim 1.6$, indicating a tendency of the system to transit to higher frequencies (see position of the green arrow in Fig. 4c). Increasing further the k -values, see the case $k = 1.3$ in Fig. 5c, the nodes occupying the transition regions, between the negative and the positive x -value domains, follow the central node (see position of the green arrow) and attain in their turn higher mean phase velocities. With a further increase in the radial coupling strength k , for example $k = 2.5$, we observe that the x state variables still traverse both the positive and negative part of the axis as in Fig. 6. Furthermore, in panel (c) we observe that all mean-phase velocities have increased as compared to lower values of k .

In the next section, sec. 5, we study how the transition from the the single

to double-well chimera takes place as we gradually increase the radial coupling strength k .

5 Dynamics with increase in the radial coupling strength

We analyze here the dynamics of the ring-star Chua network as the coupling strength k (the ray coupling strength) increases between $0 \leq k \leq 4$. The ring coupling strength is fixed as $\sigma = 0.75$. We study the behavior of the mean phase velocity of the central node, ω_{central} , of the coherent oscillators, ω_{coh} , and of the “leader” incoherent oscillator, ω_{leader} . From Fig. 5 in the previous section, we record in the incoherent regions a continuous distribution of frequencies and not a single one. In these regions we call “leader” the oscillator which demonstrates the maximum mean phase velocity, which, for this reason is called ω_{leader} . Note that there can be more than one leaders in the system, one for each incoherent region, as Fig. 5 indicates. In a way, the leader oscillators can be considered as the ones which lead the deviations from coherence, while the difference $\Delta\omega = \omega_{\text{leader}} - \omega_{\text{coh}}$ is indicative of the total incoherence in the system.

In Fig. 7 we plot the mean phase velocities of the central node ω_{central} (blue color), of the coherent nodes ω_{coh} (green color), and of the leader incoherent nodes ω_{leader} (red color). Initial conditions were chosen randomly in all simulations within the positive interval, $[0, 1]$, for the x, y, z state variables. This figure indicates the presence of a phase transition taking place in the parameter region $0.5 \leq k_{\text{trans}} \leq 1$. In particular, for small values of the radial coupling, $k \leq 0.5$, all oscillators present similar ω -values, around $\omega \sim 1$. In this region ($k \leq 0.5$), the central oscillator, $i = 1$, has the smallest frequency, slightly below the coherent ones, while the leaders have frequencies slightly above the coherent. As k increases above 0.5 the abrupt transition occurs. First the central nodes double (almost) their mean phase velocity which becomes close to 1.6, while the rest of the oscillators remain close to the values $\omega \sim 1$. This behavior holds in the intermediate coupling region, $0.5 \leq k \leq 1.0$ (for the parameter values $\sigma = 0.75$, $N = 300$ oscillators and $R = 100$ neighbors). Above this transition region, and for $k > 1$, the coherent and incoherent nodes also increase gradually their mean phase velocities, which also attain values around $\omega \sim 1.6$. In particular, for values $1.25 < k < 1.5$, the central node frequency is located between the coherent and the leader ones. When k reaches strengths > 2.0 the oscillator regions stabilize and the system attains constant frequencies, $\omega_{\text{central}} \sim 1.55$, $\omega_{\text{coh}} \sim 1.6$ and $\omega_{\text{leader}} \sim 1.72$ independent of k . The above discussion tells us that the frequency “chimera kingdom” characterized by considerable differences in the frequencies between coherent and incoherent domains is established for k -parameter values in the transition region $1.0 < k < 2.0$.

Figure 8 shows the ring-star network in action. We represent the central (blue) node, coherent (green) and incoherent (red) nodes for $k = 1$, $\sigma = 0.75$ in the ring-star network with different colors. As we see from the figure, the

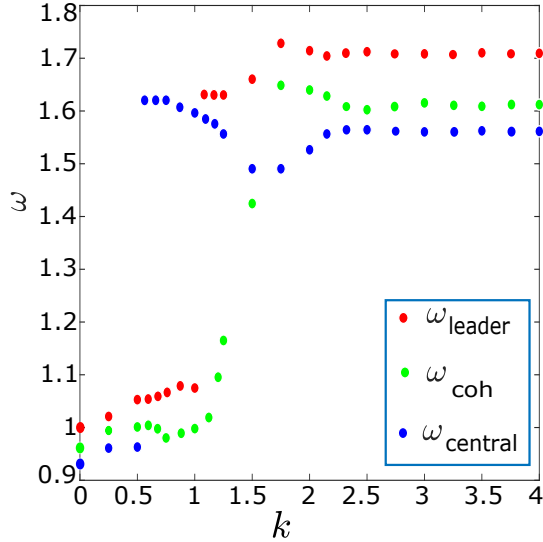


Figure 7: Mean phase velocities as a function of the coupling strength k . The mean phase velocities of the coherent nodes, ω_{coh} , are marked in green color, of the central node, ω_{central} , is marked in blue color, while the maximum mean phase velocity in the incoherent regions, ω_{leader} , is marked in red color. All other parameters as in Fig.2.

coherent nodes are not isolated but form clusters in the ring. At the same instant the incoherent nodes are most abundant.

The transition shown in Fig. 7 is corroborated by the plots depicting $\omega_{\text{central}} - \omega_{\text{coh}}$ and $\omega_{\text{leader}} - \omega_{\text{coh}}$ in Figs. 9 and 10, respectively.

Namely, in Fig. 9 we note that the values $\omega_{\text{central}} - \omega_{\text{coh}}$ remain slightly below 0, for $k < 0.5$ indicating that the central node has constantly lower frequency than the coherent nodes. Above $k > 2$, the same behavior persists. In the intermediate region, $0.5 < k < 2.0$, first the central node acquires abruptly very high frequencies for $0.5 < k < 1$, and later on its frequency gradually decreases to stabilize slightly below the frequency of the coherent nodes. We recall that, in all cases, the central node has the same characteristics (parameters) as all other nodes in the system. Concerning the leader nodes, in Fig. 10 the values $\omega_{\text{leader}} - \omega_{\text{coh}}$ remain above 0 for $k < 1.0$, demonstrating a gradual increase as a function of k in this region. They also demonstrate a delay in the transition with respect to the central node. The leaders are entrained to transit for $k \sim 1.25$ while the coherent ones reach the higher frequency domain after $k \sim 1.5$. Above $k > 2$, the leaders keep a constant small mean phase velocity difference from the coherent nodes of the order ~ 0.05 .

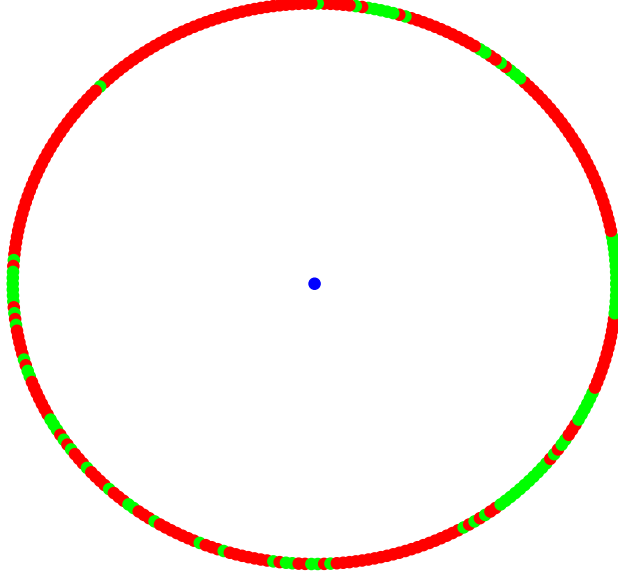


Figure 8: Coherence circle plot. The coherent nodes are marked with green, incoherent nodes are marked with red color. The number of nodes depicted here is $N = 300$. The central node is marked with blue color. The coupling strengths are fixed as: $k = 1$ and $\sigma = 0.75$. All other parameters as in Fig.2.

To study further the inhomogeneity of frequencies in the system we compute the ratio of coherent, r_{coh} and incoherent nodes r_{incoh} as a function of k , excluding the central one. The ratios of coherent and incoherent elements were calculated using Eqs. (4) and (6) and the results are depicted in Figs. 11 and 12, respectively. We have a similar picture of the transition from small to large frequency values with increasing the strength k of radial coupling. For small ($k < 0.5$) and large ($k > 2$) radial coupling strengths the ratio of coherent elements stays low, $r_{\text{coh}} \sim 0.1$ and the ratio of incoherent stays large, $r_{\text{incoh}} \sim 0.9 = 1 - r_{\text{coh}}$. In the intermediate region, $0.5 < k < 2$ a transitive behavior is recorded, where the coherent ratio increases, while the incoherent one decreases. This reorganization of the system taking place in the intermediate k regions where the frequency chimera states prevail, marks the passage from the lower to the higher frequency domain.

As a general conclusion, in the transition between low and high frequencies, first the central node makes the jump to the higher frequencies at $k \sim 0.5$ entraining the rest of the nodes. Following the central node the incoherent

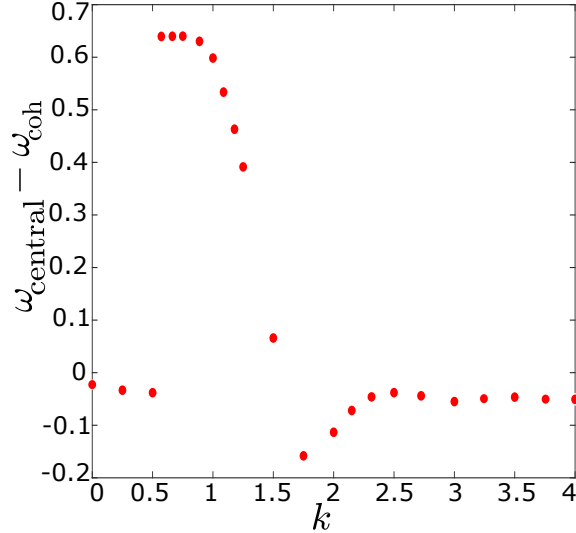


Figure 9: The difference $\omega_{\text{central}} - \omega_{\text{coh}}$ as a function of the radial coupling strength k . Ring coupling strength $\sigma = 0.75$ and other parameters as in Fig. 4.

nodes are entrained. Their leaders make the transition at $k \sim 1$, while the coherent nodes attain the transition at $k \sim 1.5$. Note that the present values are indicative and hold for the working parameter set. For different parameters (σ, N, R) , the transition values as well as the transition regions are expected to vary depending on these parameters.

6 Conclusions

We have studied a ring network of Chua circuits, equipped with a central node which serves to redistribute to the peripheral nodes information about the mean field state of all nodes. For small values of the radial coupling strengths single-well amplitude chimeras are observed. At intermediate radial couplings a transition region is observed where the frequency chimeras prevail with a large difference in the frequencies between coherent and incoherent nodes. This region mediates the transition between the lower and higher frequency domains. For large radial coupling strengths, the system attains the higher frequency domain and keeps constant mean phase velocities and ratios of coherent to incoherent nodes, independent of the radial coupling range. The frequency chimera kingdom is established for the intermediate radial couplings k -values, as evidenced by the plots of all different synchronization measures.

The above results have potential applications in the control of Chua net-

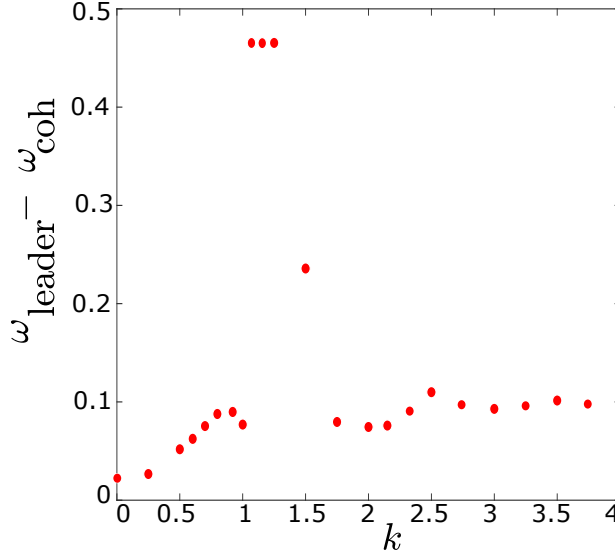


Figure 10: The difference $\omega_{\text{leader}} - \omega_{\text{coh}}$ as a function of the radial coupling strength k . Ring coupling strength $\sigma = 0.75$ and other parameters as in Fig. 4.

works as well as other coupled chaotic dynamical systems. By just adding one central node, identical to all peripheral ones, and without further modifications to the individual oscillators or to the network parameters, it is possible to entrain the system to lower or higher frequency domains as desired by the particular applications by only adjusting the radial coupling. We must stress here that the transition described above is an example of transitions taking place in nonequilibrium systems (nonequilibrium transitions); the Chua system (1) is a characteristic example of such systems since it presents chaotic, nonconservative dynamics [32, 33, 34, 39, 44]. This transition cannot be directly related to the known phase transitions in equilibrium systems at criticality, such as the Ising model phase transitions (see reference [58]).

For future studies, it would be interesting to understand how the dynamics of the Chua network changes with different coupling forms such as conjugate coupling or mean-field coupling, or by strengthening the role of the central node and endowing it with interactions to the peripheral nodes using all three x , y and z variables. Transitions in different network types may also be considered as, for example, in the case of a 2D lattice of Chua oscillators equipped with a central element, or extensions to Chua circuits in multilayer arrangements.

A different study concerns the connection between star and ring-star networks. In order to achieve a complete star network (central node connected to peripheral nodes and no connection in between the peripheral nodes), mathe-

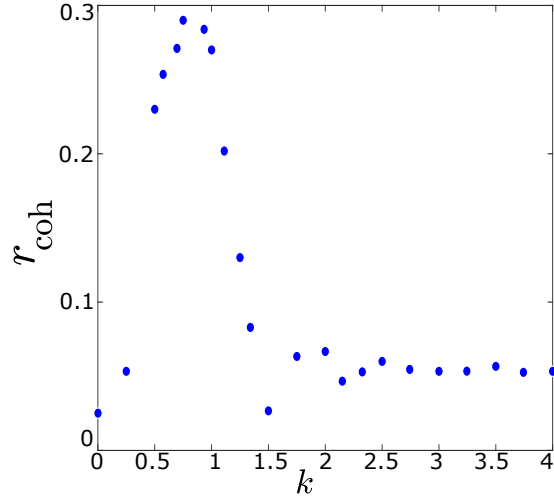


Figure 11: Ratio of coherent elements as a function of the central coupling range k . All other parameters are as in Fig. 2.

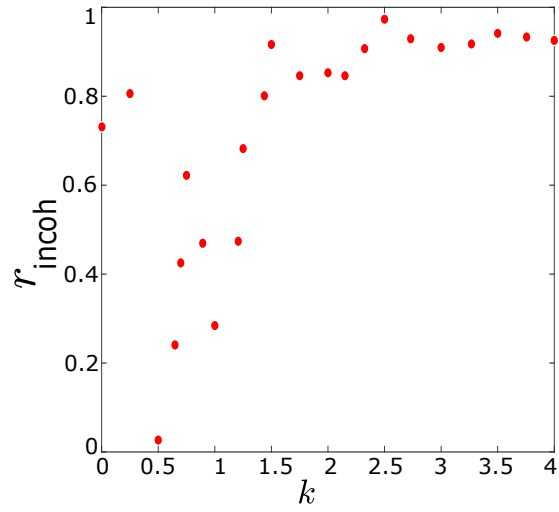


Figure 12: Ratio of incoherent elements as a function of the central coupling range k . All other parameters are as in Fig. 2.

matically we need to fix a finite value of k while letting $\sigma \rightarrow 0$. It would be interesting to account for chimera states and potential transitions in this limiting σ case and to investigate the link to the phenomenon of Remote Synchronization (RS) [56, 59], a nontrivial phenomenon in star networks, where the peripheral oscillators synchronize (without being directly linked), while the central, relay node remains asynchronous.

Acknowledgements

This work was supported by computational time granted from the Greek Research & Technology Network (GRNET) in the National HPC facility - ARIS - under project CoBrain4 (project ID: PR007011).

References

- [1] Y. Kuramoto and D. Battogtokh, Coexistence of coherence and incoherence in nonlocally coupled phase oscillators, *Nonlinear Phenomena in Complex Systems*, **5(4)**, 380 (2002).
- [2] Y. Kuramoto, Reduction methods applied to nonlocally coupled oscillator systems, in *Nonlinear Dynamics and Chaos: Where do we go from here?*, Edts. S.J. Hogan and A.R. Champneys and A.R. Krauskopf and M. di Bernardo and R. Eddie Wilson and H.M. Osinga and M.E. Homer, 209-227, CRC Press (2002).
- [3] M.J. Panaggio and D. Abrams, Chimera states: Coexistence of coherence and incoherence in networks of coupled oscillators, *Nonlinearity*, **28**, R67-R87 (2015).
- [4] E. Schöll, Synchronization patterns and chimera states in complex networks: Interplay of topology and dynamics, *European Physical Journal – Special Topics*, **225**, 891-919 (2016).
- [5] S. Majhi, B.K. Bera, D. Ghosh and M. Perc, Chimera states in neuronal networks: A review, *Physics of Life Reviews*, **28**, 100-121 (2019).
- [6] O.E. Omel'Chenko, The mathematics behind chimera states, *Nonlinearity*, **31**, R121 (2018).
- [7] A. Buscarino, M. Frasca, L.V. Gambuzza and P. Hövel, Chimera states in time-varying complex networks. *Physical Review E*, **91** 022817, (2015).
- [8] E.A. Martens, C.R. Laing and S.H. Strogatz, Solvable model of spiral wave chimeras. *Physical Review Letters*, **106**, 234102, (2011).
- [9] A. Zakharova, M. Kapeller and E. Schöll, Amplitude chimeras and chimera death in dynamical networks, *Journal of Physics:Conference Series*, **727**, 012018, (2016).

- [10] I. Omelchenko, A. Provata, J. Hizanidis, E. Schöll and P. Hövel, Robustness of chimera states for coupled FitzHugh-Nagumo oscillators. *Physical Review E*, **97** 022201 (2015).
- [11] J. Hizanidis, V.G. Kanas, A. Bezerianos and T. Bountis, Chimera states in networks of nonlocally coupled Hindmarsh-Rose neuron models. *International Journal of Bifurcations and Chaos*, **24**, 1450030 (2014).
- [12] A. Schmidt, T. Kasimatis, J. Hizanidis, A. Provata and P. Hövel, Chimera patterns in two-dimensional networks of coupled neurons. *Physical Review E*, **95**, 032224 (2017).
- [13] N.D. Tsigkri-DeSmedt, J. Hizanidis, P. Hövel and A. Provata, Multi-chimera states in the Leaky Integrate-and-Fire model. *European Physical Journal B*, **90**, 139, (2017).
- [14] E.M. Arumugam and M.L. Spano, A chimeric path to neuronal synchronization, *Chaos*, **25**, 013107, (2015).
- [15] F. Mormann, K. Lehnertz, P. David and C.E. Elger, Mean phase coherence as a measure for phase synchronization and its application to the EEG of epilepsy patients, *Physica D*, **144**, 358 (2000).
- [16] F. Mormann, T. Kreuz, R.G. Andrzejak, P. David, K. Lehnertz, P. David and C.E. Elger, Epileptic seizures are preceded by a decrease in synchronization., *Epilepsy Res.*, **53**, 173 (2003).
- [17] R.G. Andrzejak, C. Rummel, F. Mormann and K. Schindler, All together now: Analogies between chimera state collapses and epileptic seizures, *Scientific Reports*, **6** 23000 (2016).
- [18] P.J. Uhlhaas and W. Singer, Neural synchrony in brain disorders: relevance for cognitive dysfunctions and pathophysiology, *Neuron*, **52**, 155-68 (2006).
- [19] E. Tognoli and J.S. Kelso, The metastable brain. *Neuron*, **1**, 35-48, (2014).
- [20] N.C. Rattenborg, C.J. Amlaner and S.L. Lima, Behavioral, neurophysiological and evolutionary perspectives on unihemispheric sleep, *Neuroscience and Biobehavioral Reviews*, **24**, 817-842 (2000).
- [21] N.C. Rattenborg, Do birds sleep in flight?, *Naturwissenschaften*, **93**, 413-425 (2006).
- [22] L. Ramlow, J. Sawicki, A. Zakharova, J. Hlinka, J.C. Claussen and E. Schöll, Partial synchronization in empirical brain networks as a model for unihemispheric sleep, *Europhysics Letters*, **126**(5), 50007 (2019).
- [23] E.A. Martens, S. Thutupalli, A. Fourrière and O. Hallatschek, Chimera states in mechanical oscillator networks, *Proceedings of the National Academy of Sciences*, **110**, 10563-10567 (2013).

- [24] A.M. Hagerstrom, T.E. Murphy, R. Roy, P. Hövel, I. Omelchenko and E. Schöll, Experimental observation of chimeras in coupled-map lattices, *Nature Physics*, **8**, 658 (2012).
- [25] L.V. Gambuzza, A. Buscarino, S. Chessari, L. Fortuna, R. Meucci and M. Frasca, Experimental investigation of chimera states with quiescent and synchronous domains in coupled electronic oscillators, *Physical Review E*, **90**, 032905 (2014).
- [26] L. V. Gambuzza, L. Minati and M. Frasca, Experimental observations of chimera states in locally and non-locally coupled Stuart-Landau oscillator circuits, *Chaos, Solitons, Fractals*, **138**, 109907 (2020).
- [27] M.R. Tinsley, S. Nkomo and K. Showalter, Chimera and phase-cluster states in populations of coupled chemical oscillators, *Nature Physics*, **8**, 662–665 (2012).
- [28] M. Wickramasinghe and I.Z. Kiss, Spatially organized dynamical states in chemical oscillator networks: Synchronization, dynamical differentiation and chimera patterns, *PLoS ONE*, **8(11)**, e80586 (2013).
- [29] D. Wilson, S. Faramarzi, J. Moehlis, M.R. Tinsley and K. Showalter, Synchronization of heterogeneous oscillator populations in response to weak and strong coupling, *Chaos*, **28**, 123114 (2018).
- [30] J. Hizanidis, N. Lazarides and G.P. Tsironis, Robust chimera states in SQUID metamaterials with local interactions, *Physical Review E*, **94(3)**, 032219 (2016)
- [31] J. Hizanidis, N. Lazarides and G.P. Tsironis, Pattern formation and chimera states in 2D SQUID metamaterials, *Chaos*, **30(1)**, 013115 (2020).
- [32] L.O. Chua, The Genesis of Chua’s circuit, *Archiv für Elektronik und Übertragungstechnik*, **46(3)** 250–257, (1992).
- [33] T. Matsumoto, L. O. Chua and M. Komuro, The Double Scroll, *IEEE Transactions on Circuits and Systems*, **32 (8)** 797–818, (1985).
- [34] R. Lozi, Secure communications via chaotic synchronization in Chua’s circuit and Bonhoeffer-Van der Pol equation: numerical analysis of the errors of the recovered signal, *Proceedings of ISCAS’95 - International Symposium on Circuits and Systems*, **1**, 684-687, (2002).
- [35] J. Borenstein and Y. Koren, Error eliminating rapid ultrasonic firing for mobile robot obstacle avoidance, *IEEE Transactions on Robotics and Automation*, **11(1)**, 132-138, (1995).
- [36] B. Ando, S. Baglio, S. Graziani and N. Pitrone, CNNS for noise generation in dithered transducers, *Proceedings of the 17th IEEE Instrumentation and Measurement Technology Conference*, **2**, 1071-1076, (2000).

- [37] E. Bilotta, S. Gervasi and P. Pantano, Reading complexity in Chua's oscillator through music part I: A new way of understanding chaos, *International Journal of Bifurcation and Chaos*, **15**, 253-382, (2005).
- [38] B. Baird, M.W. Hirsch and F. Eeckman, A neural network associative memory for handwritten character recognition using multiple Chua characters, *IEEE Transactions on Circuits and Systems II: Analog and Digital Signal Processing*, **40**, 667-674, (1993).
- [39] L. Fortuna, M. Frasca and M.G. Xibilia, Chua's circuit implementations yesterday, today and tomorrow, *World Scientific Series on Nonlinear Science Series A, vol. 65*, World Scientific, Singapore (2009).
- [40] L.G. Roberts and B.D. Wessler, Computer network development to achieve resource sharing, *AFIPS '70 (Spring)*, 543-549, (1970).
- [41] R. Lozi, Designing Chaotic Mathematical circuits for solving practical problems, *International Journal of Automation and Computing*, **11**, 588-597, (2014).
- [42] S.S. Muni, S. Padhee and K.C. Pati, A Study on the synchronization aspect of star connected identical Chua's circuits, *2018 IEEE International Students' Conference on Electrical, Electronics and Computer Science (SCEECS)*, Bhopal, 1-6, (2018).
- [43] I.A. Shepelev, A.V. Bukh, G.I. Strelkova, T.E. Vadivasova and V.S. Anishchenko, Chimera states in ensembles of bistable elements with regular and chaotic dynamics, *Nonlinear Dynamics*, **90**, 2317-2330 (2017).
- [44] A.P. Muñozuri, V.P. Muñozuri, V.P. Villar, L.O. Chua, Spiral waves on a 2-D array of nonlinear circuits, *IEEE Transactions on circuits and systems-I: fundamental theory and applications*, **40**, 11, (1993).
- [45] A. Pikovski, M. Rosenblum and J. Kurths, Synchronization: A Universal Concept in Nonlinear Sciences, Cambridge University Press, Cambridge, 2001.
- [46] N. Kouvaris and A. Provata and D. Kugiumtzis, Detecting synchronization in coupled stochastic ecosystem networks, *Physics Letters A*, **374**, 507-515 (2010).
- [47] X.W. Hou, M.F. Wan and Z.Q. Ma, Dynamical correlations of negativity and entropy for pure and mixed states in two coupled quartic oscillators, *European Physical Journal D*, **62**, 279-288 (2011).
- [48] M.S. Baptista, R.M. Rubinger, E.R. Viana, J.C. Sartorelli, U. Parlitz and C. Grebogi, Mutual information rate and bounds for it, *PLoS ONE*, **7**, e46745 (2012).

- [49] M.C. Soriano, G. Van der Sande, I. Fischer and C.R. Mirasso, Synchronization in simple network motifs with negligible correlation and mutual information measures, *Physical Review Letters*, **108**, 134101 (2012).
- [50] S. Majhi, M. Perc and D. Ghosh, Chimera states in uncoupled neurons induced by a multilayer structure, *Scientific Reports*, **6**, 39033 (2016).
- [51] P. Kundu, P. Khanra, C. Hens and P. Pal, Optimizing synchronization in multiplex networks of phase oscillators, *Europhysics Letters*, **129**, 30004 (2020).
- [52] C. Bick and E. A. Martens, Controlling chimeras, *New Journal of Physics*, **17**, 033030 (2015).
- [53] N. Deschle, A. Daffertshofer, A. Battaglia and E.A. Martens, Directed flow of information in chimera states, *Frontiers in Applied Mathematics and Statistics*, **5**, 28, (2019).
- [54] N.D. Tsigkri-DeSmedt, I. Koulterakis, G. Karakos and A. Provata, Synchronization patterns in LIF neuron networks: merging nonlocal and diagonal connectivity, *European Physical Journal B*, **91**, 1–13 (2018).
- [55] I. Omelchenko, O.E. Omel'chenko, P. Hövel and E. Schöll, When nonlocal coupling between oscillators becomes stronger: Patched synchrony or multi-chimera states, *Physical Review Letters*, **110**, 224101, (2013).
- [56] A. Sharma, M. D. Shrimali, A. Prasad, R. Ramaswamy and U. Feudel, Phase-flip transition in relay-coupled nonlinear oscillators, *Physical Review E* **84**, 016226 (2011).
- [57] S. Ulonska, I. Omelchenko, A. Zakharova and E. Schöll, Chimera states in networks of Van der Pol oscillators with hierarchical connectivities, *Chaos*, **26**, 094825 (2016).
- [58] H.E. Stanley, Introduction to phase transitions and critical phenomena, Oxford University Press, Inc., Oxford 1971.
- [59] A. Bergner, M. Frasca, G. Sciuto, A. Buscarino, E. J. Ngamga, L. Fortuna, and J. Kurths, Remote synchronization in star networks, *Physical Review E*, **85**, (2012).